Static properties of $CsNiF_3$: Comparison of numerical results, experimental data, and predictions from soliton-bearing models

T. Delica*
Institut für Theoretische Physik, Universität Erlangen–Nürnberg, Staudtstrasse 7, W-8520 Erlangen, Germany

W. J. M. de Jonge and K. Kopinga
Department of Physics, Eindhoven University of Technology, P.O. Box 513, NL-5600 MB Eindhoven, The Netherlands

H. Leschke
Institut für Theoretische Physik, Universität Erlangen–Nürnberg, Staudtstrasse 7, W-8520 Erlangen, Germany

H. J. Mikeska
Institut für Theoretische Physik, Universität Hannover, Appelstrasse 2, W-3000 Hannover 1, Germany
(Received 7 March 1991)

The numerical quantum transfer-matrix method has been applied to the $s=1$ easy-plane ferromagnetic chain system $CsNiF_3$. A detailed analysis of experimental data on the static properties reveals that the generally accepted spin Hamiltonian for this compound gives an accurate description of the individual chains for $J/k_B=25$ K and $D/k_B=7.7$ K. At temperatures up to several degrees Kelvin above the three-dimensional ordering temperature, deviations between theory and experiment are found that are attributed to the coupling between the chains. A comparison of the quantum-transfer-matrix-method results with various analytic results supports the description of solitary excitations in $CsNiF_3$ by the classical sine-Gordon model, extended to include spin fluctuations out of the easy plane and quantum effects.

I. INTRODUCTION

One-dimensional magnetic systems with a dominant nearest-neighbor spin-spin interaction have attracted considerable attention during the last decades, both theoretically and experimentally. A number of studies have revealed that, apart from linear excitations, in these systems nonlinear excitations contribute significantly to the static and dynamic properties. Exact descriptions of the quantum chain systems, however, are still lacking.

In this context the quasi-one-dimensional compound $CsNiF_3$ has been extensively studied. From a variety of experimental investigations,[1–8] it was deduced that the individual chains in this compound can be represented by the spin Hamiltonian

$$H=-J\sum_n \mathbf{S}_n\cdot\mathbf{S}_{n+1}+D\sum_n (S_n^z)^2-g\mu_B\mathbf{B}\cdot\sum_n \mathbf{S}_n \ , \qquad (1)$$

where J represents the (ferromagnetic) intrachain exchange interaction, D the (easy-plane) single-ion anisotropy, and $\mathbf{B}$ the applied magnetic field. Approximate predictions for the static properties of chain systems described by this equation have been obtained from numerical calculations, such as extrapolating the results for finite chains[9,10] and quantum Monte Carlo techniques.[11]

The Hamiltonian (1) defines a widely used model for soliton-bearing magnetic chains.[12–17] Detailed theories of solitary excitations in these systems (as well as in systems with different symmetries) are usually based on the treatment of the Hamiltonian in the classical limit, which, of course, is in strong contrast to the fact that the spin quantum number of the magnetic ions is $s=1$. The classical picture allows one to develop a physical and intuitive picture of these excitations, which is to a large extent based on the results of large anisotropies D (which is identical to the sine-Gordon limit), whereas various estimates show that a perturbative inclusion of quantum effects should give meaningful results.[12–14] Nevertheless, efforts to obtain accurate results for experimentally accessible soliton-related properties have for many years been hampered by the difficulties in treating quantitatively a spin chain with $s=1$.

Recently, the numerical quantum transfer-matrix method (QTM) (see Ref. 18 and references therein) has been applied to the ferromagnetic $s=\frac{1}{2}$ easy-plane system $[C_6H_{11}NH_3]CuBr_3$. A very good description of the experimentally observed static properties of this compound was obtained.[19] In this paper we will present results of the $s=1$ version of this QTM and compare these with both relevant experimental data on $CsNiF_3$ and corresponding predictions for soliton-bearing model systems.

The organization of the paper is as follows. In Sec. II we will briefly outline how the static properties of the spin chain described by Eq. (1) have been calculated by the QTM. In Sec. III we will compare results of these calculations with different sets of experimental data on $CsNiF_3$, in order to deduce accurate values of the parameters J and D and to obtain detailed information on the validity of the description of this compound by the Hamiltonian (1). In Sec. IV the QTM results will be compared with corresponding predictions from classical transfer-kernel calculations and the sine-Gordon model, extended

by including spin fluctuations out of the easy plane and quantum effects. This will provide us with some information about the applicability of the soliton picture to a real $s=1$ system. The paper will be concluded in Sec. V.

II. NUMERICAL METHOD

The numerical results on static properties of the system described by the Hamiltonian (1) have been obtained by the quantum transfer-matrix method as described in detail in Ref. 18.

For spin quantum number $s=1$ and general values of the parameters J and D and **B**, we had to calculate the elements of the local 9×9 transfer matrix $\langle\sigma\sigma';\alpha|V((k_BT\mathcal{M})^{-1};\alpha)|\sigma''\sigma''';\alpha\rangle$ numerically (see also Ref. 20). All calculations have been performed for an open chain of $N=150$ sites and Trotter numbers up to $\mathcal{M}=6$. While upon increasing the chain length beyond $N=150$ the results are not found to change significantly (see also Refs. 18 and 19) at all temperatures considered, the restriction to $\mathcal{M}\leq6$, as is enforced by the limited computer storage, prevents the QTM from providing reliable data at very low temperatures. Our final results are obtained from extrapolating the results for $\mathcal{M}=4,5,6$ to $\mathcal{M}=\infty$ using the $1/\mathcal{M}^2$ rule.[21,18]

The applicability of the QTM with $\mathcal{M}\leq6$ for parameter values appropriate to $CsNiF_3$ was questioned in Ref. 11, because the "errors due to a finite value of $\mathcal{M}$ in the Trotter approximation should scale with the parameter $Js^2/\mathcal{M}k_BT$." However, confirming previous observations[20,22] for spin-1 chains, we have found very good convergence in the temperature region where the majority of the experimental data on $CsNiF_3$ have been collected. Typically, results from extrapolations for $\mathcal{M}=3,4,5$ agreed within 5% with results from extrapolations for $\mathcal{M}=4,5,6$ down to $T=4$ K (heat capacity, susceptibility) or $T=3$ K (magnetization). Moreover, our results agree fairly well with the Monte Carlo data for the magnetization obtained in Ref. 11 with Trotter numbers up to $\mathcal{M}=12$, as indicated in Fig. 1(a). Figure 1(b) reveals that the Monte Carlo data for the excess heat capacity ΔC display a considerable scatter. In addition, at $T=7$ K the Monte Carlo data seem to deviate systematically from the QTM results.

The very good convergence on the one hand and the satisfactory agreement with Monte Carlo data for the magnetization on the other hand can be explained by the following two arguments. First, the real-space decomposition used in our calculations is known to be superior[20] to the checkerboard decomposition as applied in Ref. 11 and therefore can compensate for smaller values of $\mathcal{M}$. Second, the requirement of a small value of the above quoted parameter in order to guarantee good convergence in the calculation of expectation values is too restrictive, because it does not take into account the fact that the noncommutativity of the involved operators becomes unimportant in the classical limit $s\rightarrow\infty$. With respect to the excess heat capacity ΔC, we do not consider the above-mentioned deviations of the Monte Carlo data from the QTM results to be significant. This is not only because of the large scatter in the Monte Carlo data, but also due to the observation[23,19] that ΔC (for spin-$\frac{1}{2}$ chains) may be underestimated by numerical calculations within the checkerboard decomposition for finite $\mathcal{M}$.

In the following we list some further details of our numerical procedure. The heat capacity $C\equiv dE/dT$ and the susceptibility $\chi^{\alpha\alpha}\equiv dM^\alpha/dB^\alpha$ along $\alpha=x,y,z$ have been obtained by a numerical differentiation of the results for the internal energy $E\equiv\langle H\rangle/N$ and the magnetization $M^\alpha\equiv g\mu_B\sum_n\langle S_n^\alpha\rangle/N$, respectively.[24] Assuming that in zero field the spin-spin correlations $\langle S_0^\alpha S_n^\alpha\rangle$ decay exponentially for large distance n, we have calculated the inverse correlation length κ_α by appealing to the formula[25]

$$(\kappa_\alpha)^2=2\lim_{N\rightarrow\infty}\left[\sum_{n=-N/2}^{N/2}\langle S_0^\alpha S_n^\alpha\rangle\Big/\sum_{n=-N/2}^{N/2}n^2\langle S_0^\alpha S_n^\alpha\rangle\right]. \tag{2}$$

For details of the actual evaluation, see Ref. 19. Similarly, we have calculated the static structure factor at wave number q in the presence of a nonzero field by appealing

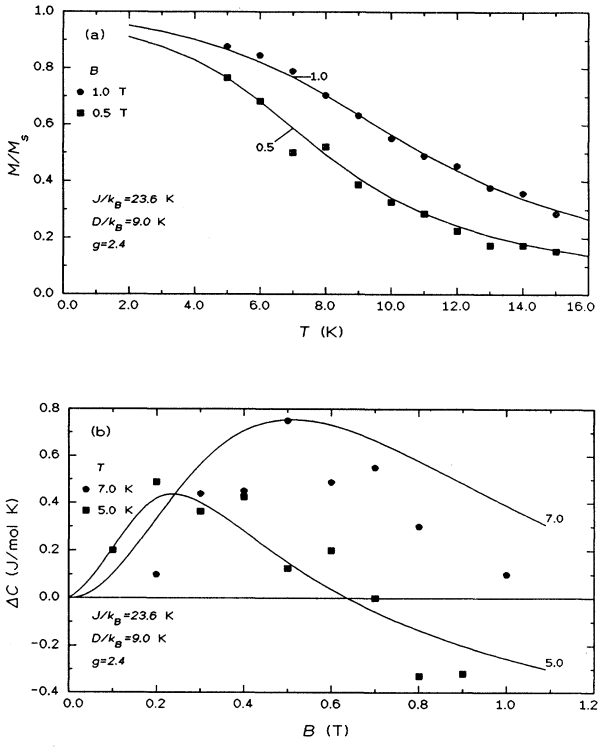

FIG. 1. (a) Temperature dependence of the magnetization and (b) field dependence of the excess heat capacity per spin of the model described by Eq. (1) with the field in the easy plane. Numbers attached to the curves correspond to the field values (in units of T) and temperature values (in units of K), respectively. QTM results are represented by solid curves; data points denote Monte Carlo results from Ref. 11. In these plots the parameter values are $J/k_B=23.6$ K, $D/k_B=9$ K, and $g=2.4$.

to the formula

$$\mathcal{S}^{\alpha\alpha}(q)=\frac{1}{2\pi}\lim_{N\to\infty}\sum_{n=-N/2}^{N/2}\exp(iqn)(\langle S_0^{\alpha}S_n^{\alpha}\rangle-\langle S_0^{\alpha}\rangle^2)\ . \tag{3}$$

The numerical results for the classical version of the model described by Eq. (1), to be presented in Sec. IV, have been obtained by the classical transfer-kernel method (CTM).[26–29]

III. COMPARISON OF EXPERIMENTAL DATA TO QTM RESULTS

In this section we will present a direct comparison of observed static properties of $CsNiF_3$ with results of the QTM calculations outlined in the preceding section. For a meaningful comparison of numerical predictions with available experimental data, the spin Hamiltonian and relevant parameters of $CsNiF_3$ should be accurately known. On the other hand, no information is required about the underlying physical processes in terms of elementary excitations. Note that this is complementary to the next section, where we compare the QTM results with predictions from soliton-bearing model systems. Such a comparison, in principle, can be done for arbitrarily chosen values of parameters.

Several estimates for the values of g, the exchange parameter J, and the easy-plane anisotropy parameter D [cf. Eq. (1)] have been reported.[4,5,7] The accuracy of these values, however, is not quite clear, since they often have been obtained from a description of experimental results by approximate theoretical calculations. Apart from this, we like to stress that Eq. (1) describes a purely one-dimensional (1D) system, whereas in the actual experimental system 3D effects due to the interchain coupling may be important, especially at low fields and temperatures, where eventually 3D long-range order is induced. Therefore, we will use a strategy where we deduce the parameter values from static properties for which accurate experimental data are available (under conditions where 3D effects are small) and for which the convergence of the QTM results in the Trotter number $\mathcal{M}$ is particularly good, such as the magnetization. Next, we will use this set of values in the calculation of other properties, such as the excess heat capacity and spin-spin correlations.

A. Magnetization and susceptibility

Experimental data on the magnetization of $CsNiF_3$ have been reported[7] for external fields up to 1 T within the easy plane. Since, in general, small deviations from ideal model behavior are expected to be less significant at higher fields, we have supplemented these results with measurements for $1.2\ \mathrm{K}<T<20\ \mathrm{K}$ at fields up to 5 T within the easy plane and up to 3 T perpendicular to it. The data were collected using a commercial vibrating-sample magnetometer. The absolute accuracy of the observed magnetization is better than 4%, whereas the relative deviations are about 1%. No demagnetization corrections were applied, since they amount to at most 0.01 T. Temperature readings were obtained from a calibrated carbon-glass thermometer and reflect the actual sample temperature within 50 mK. The temperature could be controlled with a typical stability of 20 mK at 1.5 K, gradually decreasing to 100 mK around 20 K.

The measurements for external fields within the easy plane ($\mathbf{B}\perp\mathbf{c}$) were collected using two single crystals with a mass of 14.5 and 18.0 mg, respectively. At 1.2 K, saturation could be reached at the highest fields. From the observed magnitude of the saturation magnetization $M_s=g\mu_B$, a value of $g=2.1\pm0.05$ was deduced, which compares reasonably well with the various results quoted in the literature.[1,5–7] Since the present value is obtained without any fits of model calculations to the data, the choice

$$g=2.1 \tag{4}$$

will be used as a fixed parameter in all calculations to be presented below. We will compare our QTM results with the data collected at temperatures above 4.2 K, which are plotted as M/M_s against B in Fig. 2(a).

The measurements for fields perpendicular to the easy plane ($\mathbf{B}\|\mathbf{c}$) were performed on a single crystal with a mass of 108.3 mg. For this direction of $\mathbf{B}$, the magnetization shows only a small temperature dependence below $T=7$ K. For sake of clarity, we have only included the data collected at higher temperatures in Fig. 2(b). Because of the pronounced easy-plane character of $CsNiF_3$,

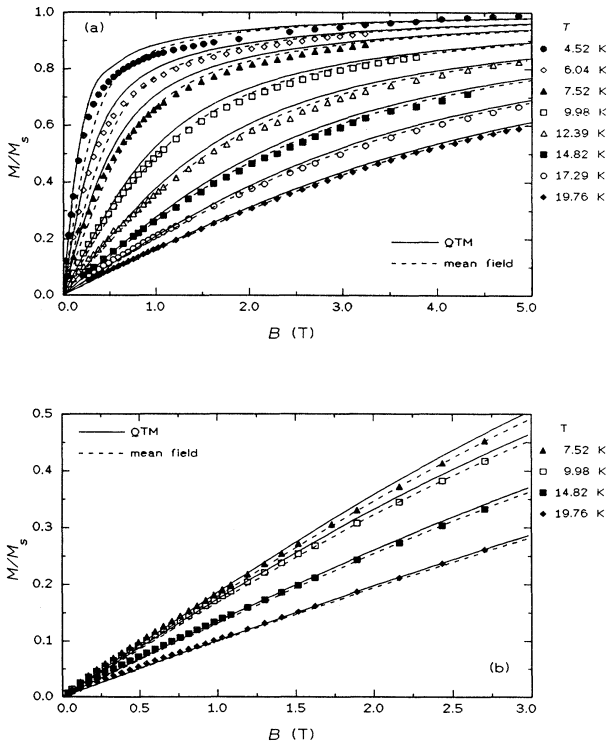

FIG. 2. Reduced magnetization M/M_s of $CsNiF_3$ for $\mathbf{B}$ (a) within or (b) perpendicular to the easy plane at various temperatures. Solid curves denote the corresponding QTM results, whereas the dashed curves reflect the inclusion of 3D effects within a mean-field approximation.

no saturation could be reached. Since, in general, both the J and g tensors of Ni^{2+} systems are fairly isotropic, we will use the value (4) inferred above also in the analysis of the data for $\mathbf{B}\|\mathbf{c}$.

Our aim in the analysis of the magnetization is to obtain a description of the experimental data for both $\mathbf{B}\|\mathbf{c}$ and $\mathbf{B}\perp\mathbf{c}$ within experimental accuracy using the same set of values for the parameters J and D. The best overall description was found for the set of values

$$J/k_B=25\ \text{K}\ ,\quad D/k_B=7.7\ \text{K}\ . \tag{5}$$

The inferred values of these parameters compare well with the values $J/k_B=23.6$ K and $D/k_B=9$ K obtained from an analysis of the magnon dispersion relation within a classical model.[4] Inclusion of quantum corrections[30] changes the latter values to $J/k_B=26$ K and $D/k_B=8$ K, yielding an even better agreement. However, some systematic deviations between theory and data for the magnetization persisted, which increased up to 5% of the saturation magnetization at lower temperatures. Since at temperatures above 4.2 K, where the analysis is performed, the numerical error in the QTM calculation of the magnetization is less than 1%, the observed deviations very likely originate from the fact that the real magnetic behavior of $CsNiF_3$ is not adequately described by the pure 1D model Hamiltonian (1). Since the interchain interactions can neither be treated analytically nor be included in the QTM calculations, we have estimated their effect by a mean-field approximation.

Experimental information about the magnitude of the interchain coupling can be obtained from the magnetic phase diagram of $CsNiF_3$, which has been deduced by neutron-diffraction experiments[2] from the field and temperature dependence of the intensity of the $(\frac{1}{2},0,0)$ Bragg reflection. At low temperatures a transition from an antiferromagnetic domain state to a ferromagnetic alignment of the chains is observed at an applied critical field $B_c=0.21$ T within the easy plane. At this field the Zeeman energy equals the (antiferromagnetic) interchain-coupling energy. Within the mean-field approximation, the interchain interactions will reduce the "effective" field at the individual chains by an amount B_cM/M_s. Consequently, the magnetization M of an individual chain in a field B_{th} is actually reached at an applied field B_0 given by

$$B_0=B_{\text{th}}+B_cM/M_s\ . \tag{6}$$

A similar correction has been applied in the description of the experimental results for fields perpendicular to the easy plane. In this case no direct experimental information on the mean-field correction is available. However, since for this field direction the magnitude of M is relatively small, the correction is also small. Hence we have taken the interchain coupling as isotropic, i.e., used Eq. (6), although it may be largely of dipolar origin.[2]

The corresponding theoretical predictions are given by the dashed curves in Fig. 2. The solid curves reflect the numerical results for the purely 1D system. Inspection of the figure reveals that the inclusion of a mean-field correction yields a nice description of the data above 0.5 T, but at lower fields the 1D model seems more appropriate. This is corroborated by the analysis of the zero-field susceptibility. In Figs. 3(a) and 3(b) we have plotted the reported data[5] for the in- and out-of-plane susceptibility, respectively. The solid curves denote the numerical results for the 1D model Hamiltonian, using the same set of parameter values as above. The dashed curves reflect the inclusion of the interchain-coupling energy $\nu J_\perp<0$, where ν denotes the effective number of neighboring chains, within a mean-field approximation. In this approach the observed 3D susceptibility χ_{3D} is related to the susceptibility χ_{1D} of an individual chain by[31]

$$\chi_{3D}\approx\chi_{1D}\left[1-\frac{\nu J_\perp}{g^2\mu_B^2}\chi_{1D}\right]^{-1}\ . \tag{7}$$

By equating the Zeeman energy at the critical field B_c and the antiferromagnetic interchain-coupling energy, this relation can be rewritten as

$$\chi_{3D}\approx\chi_{1D}(1+B_c\chi_{1D}/M_s)^{-1}\ . \tag{8}$$

From Fig. 3 it is obvious that the description of the experimental out-of-plane susceptibility by the corrected

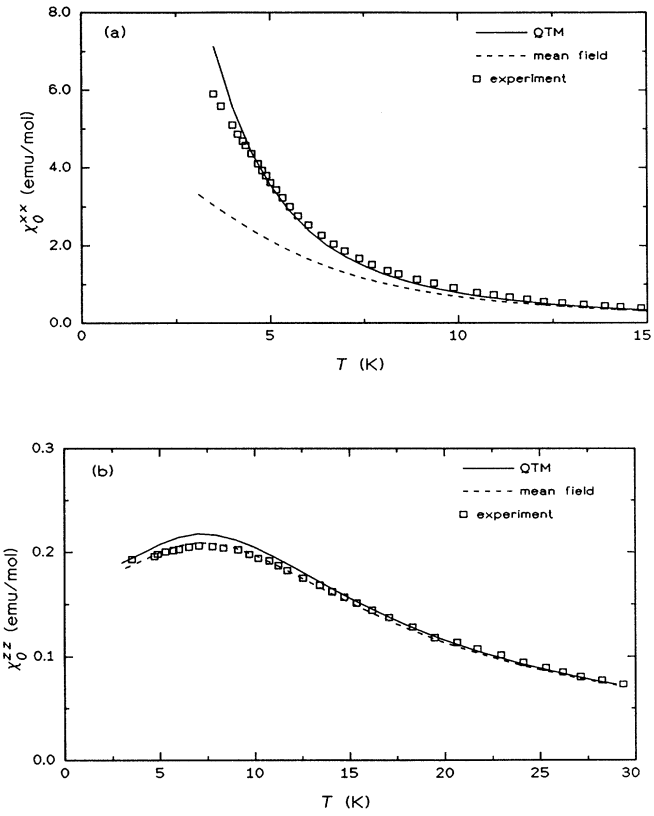

FIG. 3. Zero-field (a) in-plane and (b) out-of-plane magnetic susceptibility of $CsNiF_3$. Squares represent the experimental data taken from Ref. 5. The solid curves denote the corresponding QTM results, whereas the dashed curves reflect the inclusion of 3D effects within a mean-field approximation.

numerical results is very good. The calculated in-plane susceptibility, however, shows large deviations from the data if the mean-field correction is included. The reason for this systematic deviation, which is also present in the low-field magnetization for $\mathbf{B}\perp\mathbf{c}$, is not clear. It may be related to the observed domain structure of $CsNiF_3$ within the ordered state.[2] This structure suggests a certain degree of competition between the (long-range) dipolar and (short-range) superexchange interactions between the chains, which cannot be properly accounted for by the simple mean-field approximation used in the present analysis.

To conclude this part of the analysis, we feel confident to state that our QTM results describe the observed zero-field susceptibility and the field and temperature dependence of the magnetization in $CsNiF_3$ with an accuracy that is comparable to the uncertainty caused by the interchain interactions.

B. Heat capacity

The heat capacity of $CsNiF_3$ has been studied much more extensively than the magnetization or susceptibility. These studies have been stimulated by the observation[32] that the excess heat capacity ΔC, i.e., the heat capacity measured in the presence of an external field within the easy plane minus the zero-field heat capacity, is dominated by the contribution of nonlinear excitations. Nevertheless, comparison of experimental data on ΔC (Ref. 33) with predictions based upon the classical sine-Gordon model reveal large systematic deviations, which increase at lower fields and temperatures.

The adequacy of the classical sine-Gordon model to describe the excess heat capacity of a 1D $s=1$ easy-plane ferromagnet with the parameter values representative for $CsNiF_3$ will be discussed in Sec. IV. In this section we focus on a direct comparison of the experimental data on ΔC with results obtained from QTM calculations. For this purpose we have plotted the reported data on ΔC (Ref. 33) against the applied field B in Fig. 4. The solid curves represent the corresponding QTM results, calculated for the parameter values (4,5), inferred from the analysis of the magnetization and susceptibility. Inspection of this figure reveals only a qualitative agreement between theory and data. The maxima of the experimentally observed excess heat capacity are lower than the QTM results, the difference being larger at lower temperatures. Apart from this, the applied fields $B_{\max}$ at which these maxima occur are systematically larger than the corresponding theoretical fields by about 0.1–0.2 T.

Since in the present temperature region the uncertainty induced by the extrapolation in the Trotter number $\mathcal{M}$ (cf. Sec. II) is expected to be less than 5%, we attribute the observed discrepancies to deviations of $CsNiF_3$ from ideal model behavior or, more specifically, to the coupling between the individual chains. We can, of course, include these 3D effects within a mean-field approximation, similar to the analysis of the magnetization and susceptibility presented above. Such a procedure indeed yields a reduction of the effective field at the individual chains of roughly 0.15 T, which is sufficient to explain the observed shift of $B_{\max}$. However, it does not change the magnitude of $\Delta C(B)$ itself. In our opinion this can only be achieved by including the interchain interactions directly in the spin Hamiltonian, which, however, can no longer be treated within the present QTM formalism, as already mentioned above.

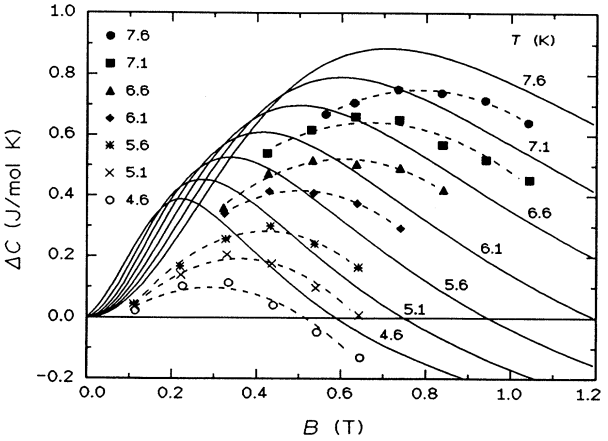

FIG. 4. Field dependence of the excess heat capacity $\Delta C = C(\mathbf{B}\perp c) - C(\mathbf{0})$ of $CsNiF_3$ at various temperatures. The symbols represent the experimental data taken from Ref. 33. The dashed curves are parabolic fits to these data. The solid curves denote the corresponding QTM results.

C. 1D spin correlations

Using quasielastic neutron scattering, it is possible to determine the spin-spin correlations within the individual chains. In $CsNiF_3$ these ferromagnetic correlations give rise to diffuse scattering with maximum intensity in planes in reciprocal space perpendicular to c^* at even values of the Miller index l, because the spin-spin distance equals $c/2$.[34] The scattering cross section along a direction normal to such a plane can be approximated by a Lorentzian[25,34]

$$\left[\frac{d\sigma}{d\Omega}\right]_\alpha = A_\alpha \mathcal{S}^{\alpha\alpha}(q) \approx \frac{A_\alpha \kappa_\alpha^2 \chi^{\alpha\alpha}}{\kappa_\alpha^2 + q^2} \ . \tag{9}$$

In this equation A_α is a proportionality factor, κ_α is the inverse correlation length for the spin components S^α, $\chi^{\alpha\alpha}$ is the magnetic susceptibility of the chain along $\alpha = x,y,z$, and q is the distance of the scattering vector to the plane. Since only spin components perpendicular to this vector contribute to the magnetic scattering, it is, in principle, possible to determine selectively the correlations between the components within or out of the easy plane, by choosing a suitable scattering configuration. We will confine ourselves to the experimental results which have been reported[35] for the in-plane components.

In Fig. 5 we have reproduced the experimentally observed maximum scattering intensity in the (0,0,2) plane at various values of the external field applied perpendicular to c^*. The scattering configuration was chosen such

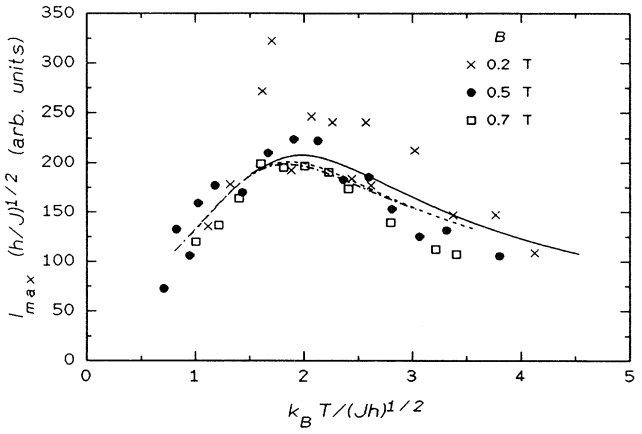

FIG. 5. Universal plot of the maximum diffuse neutron-scattering intensity in the (0,0,2) plane at various magnetic fields, where $h \equiv g\mu_B B$. The symbols represent the experimental data taken from Ref. 35. The QTM results for $B = 0.2$, 0.5, and 0.7 T are denoted by the solid, dashed, and dot-dashed curves, respectively.

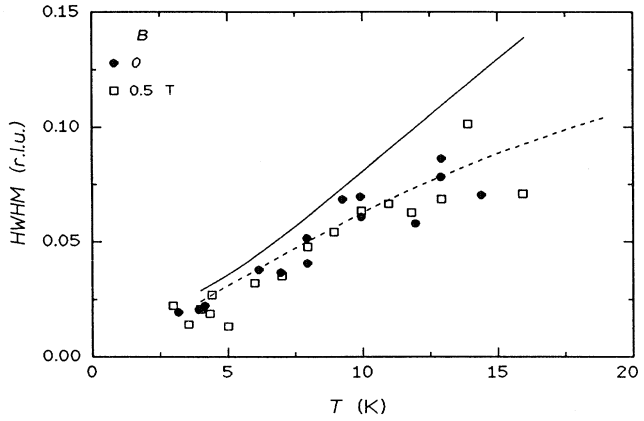

FIG. 6. Temperature dependence of the HWHM of the neutron-scattering intensity profile perpendicular to the (0,0,2) plane at $B = 0$ and 0.5 T. The symbols represent the experimental data taken from Refs. 35 and 36. The solid curve represents the QTM result for the inverse zero-field correlation length, whereas the dashed curve reflects the result of a QTM simulation of the experimental analysis (see text). The abbreviation "r.l.u." means reciprocal lattice units.

that the intensity is proportional to the sum of the in-plane susceptibilities $\chi^{\alpha\alpha}$, with $\mathbf{e}_\alpha \perp \mathbf{B}$ and $\mathbf{e}_\alpha \| \mathbf{B}$, respectively. The data are plotted in the usual "universal" way in order to check if the sets collected at different fields collapse onto a single curve. The various curves in the figure reflect the corresponding numerical QTM results for the spin Hamiltonian (1), scaled by one constant factor in the vertical direction to match the data. These results have been obtained directly from the spin-spin correlations using Eq. (3) for $q = 0$. In the calculations of $\langle S_0^\alpha S_n^\alpha \rangle$ we again used the set of paramter values (4,5). The figure reveals a very nice overall agreement between theory and data. At the lowest field of 0.2 T the experimental intensity seems somewhat higher than the theoretical prediction. Both the numerical results and data show deviations from universal behavior, in the sense that the maximum of the intensity increases at lower fields, but these deviations are very small.

Next, we will consider the correlation length. From Eq. (9) it is obvious that the inverse correlation length κ is equal to the half width at half maximum (HWHM) of the observed scattering profile $\mathcal{S}(q)$. In Fig. 6 we have plotted the reported HWHM as a function of temperature for $B = 0$ (Ref. 35) and $B = 0.5$ T.[36] As already noted by the authors of Ref. 36, the correlation length is independent of the applied field within experimental error. The solid curve reflects the calculated temperature dependence of κ for $B = 0$, using Eq. (2) and the parameter values (5).

The numerical results for κ obtained from this equation are equal to the HWHM of the calculated scattering profile $\mathcal{S}(q)$ according to Eq. (3) within a few percent, indicating that the approximation of $\mathcal{S}(q)$ by a Lorentzian [Eq. (9)] is allowed. Inspection of Fig. 6 reveals that the calculated values of κ are significantly higher than the experimental data. The difference increases at higher temperatures, where the QTM results are very accurate. On the other hand, 3D effects can be ruled out completely, since only the 1D correlations contribute to the intensity profile in the neutron-scattering experiments.

To resolve this discrepancy, we performed a numerical simulation of the experimental analysis of the measurements, in which a high-temperature ($T > 40$ K) background was subtracted from the observed intensity to obtain the purely magnetic scattering.[36] More precisely, we calculated $\mathcal{S}(q)$ at $T = 50$ K and subtracted this intensity from the scattering profile calculated for 4 K $\leq T \leq$ 20 K. The temperature dependence of the HWHM of the resulting profile is represented by the dashed curve in Fig. 6, which agrees very nicely with the experimental data. Obviously, a direct determination of the spin-spin correlation length from the observed quasielastic neutron-scattering intensity profile is very difficult when the scattering profile is broad.

IV. INTERPRETATION OF QTM RESULTS IN TERMS OF SOLITONS

As already mentioned in the Introduction, the present QTM results give the opportunity to aim at a quantitative comparison of numerical data with both experiments and approximate analytical treatments. Of course, the numerical data alone and their comparison to experiments cannot verify or falsify an underlying physical picture, but the discussion of the present results in terms of approximate analytical results (both classical and semiclassical) will allow one to draw conclusions about the relevance of the physically appealing soliton picture for a magnetic chain system with $s = 1$. This is what we aim at in this section.

The power of this effort is obviously quite different for static quantities such as the heat capacity and for dynamic quantities such as the properties of the soliton-related

central peak in the dynamic structure factor: Whereas static quantities can be compared directly to the results of the numerical calculations, the discussion of dynamic quantities will be necessarily restricted to global numbers obtained by an integration over frequency and requires some additional analysis to disentangle the different contributions to the related static quantity, which is accessible numerically to the QTM method.

A. Soliton-induced magnetic heat capacity

The discussion of the magnetic heat capacity usually starts from the fact that in the classical sine-Gordon (SG) approximation a plot of C/m vs $T/E_{\rm sol}$, where $m \equiv (g\mu_B B/Js)^{1/2}$ is the soliton mass and $E_{\rm sol} \equiv 8mJs^2$ is the soliton rest energy, gives a universal curve. It is well known from the numerical transfer-kernel calculations in Ref. 37 and from the analytical work in Ref. 38 that the final classical SG result is considerably below the result for the noninteracting one-soliton phenomenological approach (obtained in the spirit of Ref. 39), but that higher-order terms in the expansion of the free energy (power-law terms as well as one- and two-soliton terms) are necessary and sufficient to give agreement with the classical SG transfer-kernel results. Following these calculations the understanding of the magnetic heat capacity in the real magnetic chain material $CsNiF_3$ developed in the following steps.

Transfer-kernel calculations (CTM) for the classical version of the Hamiltonian (1) gave[28] a large enhancement of the heat capacity above the SG result (see also Refs. 40 and 41). Qualitatively, this was understood in the soliton description as resulting from the strong out-of-plane fluctuations for finite $\lambda \equiv 2Ds/g\mu_B B$ (finite λ gives the SG theory), predicting an increase in soliton density by a factor $\exp(3/\sqrt{\lambda})$. On the other hand, the reasonable agreement between experimental and classical SG results now appeared as fortuitous and enforced the conclusion that quantum effects must be essential for a quantitative understanding of the magnetic heat capacity. In a qualitative way, this turned out to be in agreement with semiclassical calculations: Whereas quantum corrections to the SG model did not show any significant decrease,[42,43] the combination of out-of-plane and quantum corrections[14] lead to a substantial decrease of the heat capacity and thus showed that it should be possible in principle to discuss the magnetic heat capacity in terms of the soliton picture also in the real $s=1$ spin chain.

The numerical results to be presented below give a much more quantitative picture, which is completely consistent with the "state of the art" described above. In Fig. 7 we show the results for several magnetic fields applied in the easy plane for the $s=1$ spin chain and its classical analog, both for $D/k_B = 7.7$ K. For comparison the classical SG result (universal plot for all magnetic fields) is also shown. Consistent with Ref. 28, it is seen that for the system described by the full Hamiltonian (1) the scaling property survives only approximately and that the system has a strongly enhanced heat capacity in the classical limit. On the other hand, the reduction due to quantum effects is also clearly seen and improves the description of the experimental data (cf. Fig. 4). Figure 8 demonstrates that this reduction is essentially influenced by the out-of-plane fluctuations: When we increase the strength of the single-ion anisotropy to $D/k_B = 35$ K, the ratio of classical to quantum peak heights increases.

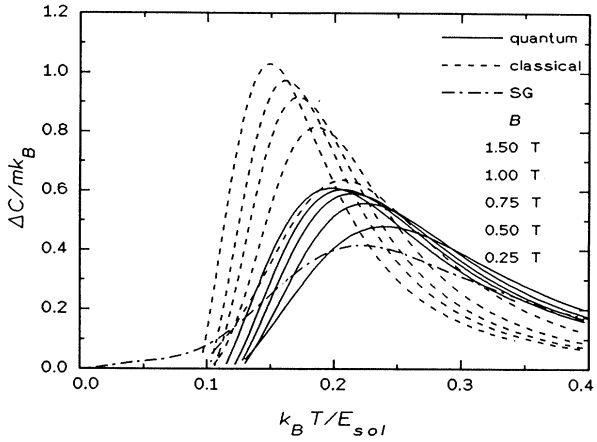

FIG. 7. Reduced excess heat capacity $\Delta C/mk_B$ vs reduced temperature $k_B T/E_{\rm sol}$ with various magnetic fields applied in the x direction. Comparison of QTM results, CTM results, and the classical SG result.

At this point we should mention that approaching the quantum sine-Gordon (QSG) model is more subtle than just increasing the anisotropy energy D in the QTM calculations, since the coupling constant of the QSG chain corresponding to the magnetic chain is $g^2 = (2D/Js^2)^{1/2}$.[44] Therefore increasing D soon brings one beyond the range of definition of the QSG system ($g^2 < 8\pi$), if the spin value s is not increased at the same

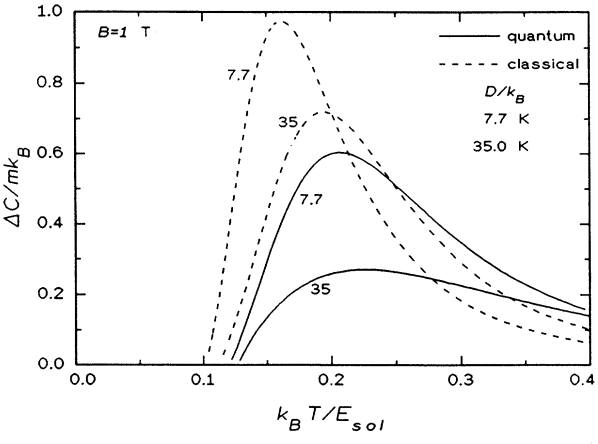

FIG. 8. Reduced excess heat capacity vs reduced temperature for different values of D reflected by the numbers attached to the curves. A field of strength 1 T is applied in the x direction.

time. This fact reflects the limitation of the mapping of the quantum magnetic chain to the QSG chain, which is valid only for $1/s \ll 1$, i.e., $g^2 \ll 1$, and thus is not compatible with diverging D.

Comparing the present numerical results to the qualitative results from semiclassical calculations based on the soliton picture described above, we conclude that an interpretation of the magnetic heat capacity in terms of solitary excitations makes sense only for the quantum chain—classical concepts make sense for a qualitative discussion (e.g., relating the maximum in the heat capacity to the soliton energy)—whereas there is no hope at present to obtain a quantitative theory showing explicitly the action of solitary excitations for the $s=1$ chain.

B. Structure factors

Whereas the heat capacity offers rather indirect information about solitary excitations in 1D magnets, the investigation of time-dependent correlation functions or dynamic structure factors leads to much more direct results about the density, spatial shape, and velocity distribution of solitons and, historically, was the basis of the first identification of solitons in $CsNiF_3$.[16] On the other hand, detailed theoretical discussions of time-dependent correlation functions turned out to be rather involved, and even complete classical results at the level of transfer-kernel calculations were not available. Therefore, the activity has shifted somewhat to simpler static quantities, such as the heat capacity, in the course of time. Using the QTM, respectively the CTM, here we present rather complete numerical results for static correlation functions or static structure factors for both the quantum and classical spin system and show that a discussion of these results consistent with the soliton picture of elementary excitations is possible.

To prepare this discussion, we start by a short survey of the various structure factors and their importance for the soliton discussion as found at the classical level (see also Ref. 17).

(1) Correlations in the easy plane parallel to the magnetic field contain both long-range order (magnetization) induced by the external field as well as longitudinal fluctuations. The latter have two important contributions, differing in their dynamical characteristics: (i) the soliton-induced central peak, which in the noninteracting soliton limit is given by

$$\mathcal{S}^{xx}_{\mathrm{sol},0}(q,\omega)=\frac{32}{cq\pi m}\left[\frac{\beta m}{\pi}\right]^{1/2} n_{\mathrm{sol}} e^{-4\beta m(\omega/cq)^2} \times\left[\frac{Q}{\sinh Q}\right]^2, \tag{10}$$

$$n_{\mathrm{sol}}\equiv 4m\left[\frac{\beta m}{\pi}\right]^{1/2} e^{-8\beta m}, \quad Q\equiv\frac{\pi q}{2m}$$

[here n_{sol} is the soliton density, $\beta\equiv Js^2/k_BT$ denotes the inverse reduced temperature, and $c\equiv(2DJs^2)^{1/2}$ is the magnon velocity] and (ii) the two-magnon contribution consisting of two parts of equal strength, one centered at zero frequency and competing with the soliton-induced central peak, the other at about twice the spin-wave energy.

(2) Correlations in the easy plane perpendicular to the magnetic field are strongly dominated (in particular for small wave numbers) by the one-spin-wave contributions to these transverse correlations. For nonzero wave numbers a soliton-related central peak is present [replace $\sinh Q$ by $\cosh Q$ in Eq. (10)].

(3) Correlations perpendicular to the easy plane have both soliton and spin-wave contributions and are interesting as an indicator of the strength of out-of-plane fluctuations, which should be considered as the basic difference between the simplifying SG description and the realistic magnetic chain.

Whereas, with very few exceptions, the discussion of soliton-related correlations so far has been restricted to the classical limit, spin-wave-related contributions in $\mathcal{S}^{xx}$ and $\mathcal{S}^{yy}$ can also be obtained in the usual quantum approach (i.e., using the appropriate variant of the Holstein-Primakoff method; see Refs. 30 and 45). To discuss the numerical results, we compare the results for the spin-1 chain to the classical results (obtained for a unit spin vector) multiplied by a factor $s(s+1)=2$ in order to have the same normalization. The most direct signature of quantum effects is the increase of out-of-plane fluctuations, which is shown in Fig. 9. This figure shows quantitatively how the effective in-plane spin component becomes smaller, implying a corresponding decrease of both

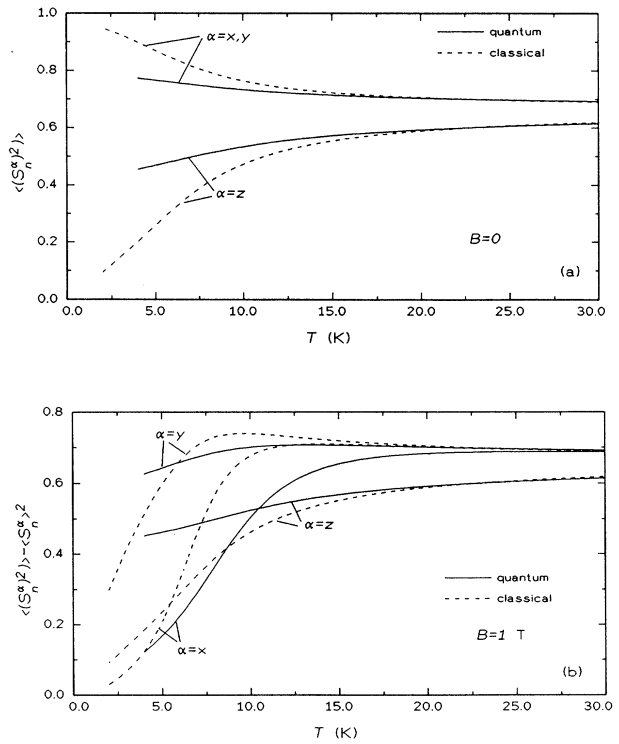

FIG. 9. Temperature dependence of the autocorrelations $\langle (S^\alpha)^2 \rangle - \langle S^\alpha \rangle^2$ (a) in zero field and (b) in a field of strength 1 T applied in the x direction.

soliton-induced and spin-wave-related in-plane correlation functions. For a more detailed discussion, we concentrate on $\mathcal{S}^{xx}(0)$. In Fig. 10(a) the variation with temperature of this quantity is shown for a magnetic field of 1 T along the x axis and an anisotropy of $D/k_B=7.7$ K, both for the $s=1$ chain and in the classical limit. The overall behavior in these two cases is similar; introducing quantum mechanics lowers the maximum by about 20% and shifts the maximum to higher temperatures. Varying the parameters, the following variations are observed: Changing D/k_B to 35 K, we find in the classical limit little change for low temperatures and a definite increase for higher temperatures. The latter is consistent with a suppression of out-of-plane fluctuations with larger anisotropies, leading to larger in-plane components. For a magnetic field of 0.5 T, the curves are qualitatively similar, apart from the expected general shift to lower temperatures. The classical SG transfer-kernel results (as extrapolated from Ref. 37) lie somewhat (10–20%) below the CTM results for the classical spin chain with $D/k_B=7.7$ K. As a whole, $\mathcal{S}^{xx}(0)$ as a static quantity has the same qualitative behavior as the heat capacity: an increase due to out-of-plane fluctuations at the classical level and a compensating decrease upon the introduction of quantum effects. Quantitatively, these changes are much less spectacular than for the heat capacity.

With respect to soliton-induced properties, the most interesting question is whether it is possible to decompose the global result for $\mathcal{S}^{xx}(0)$ into soliton and two-magnon

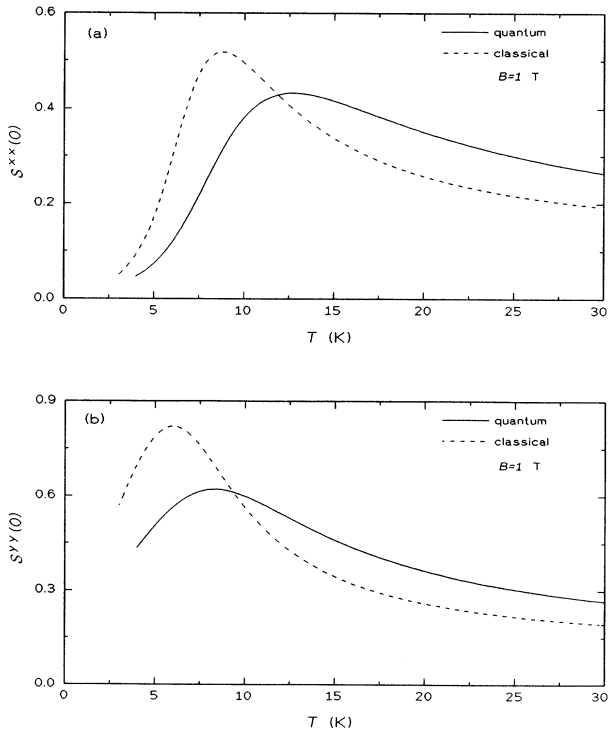

FIG. 10. Temperature dependence of the static structure factor at zero wave number $\mathcal{S}^{\alpha\alpha}(0)$ (a) for $\alpha=x$ and (b) for $\alpha=y$. A field of strength of 1 T is applied in the x direction.

TABLE I. Contributions to the classical structure factor at zero wave number $\mathcal{S}^{xx}(0)$ with a field $B=1$ T applied along the x axis. If the numerical calculation of the soliton shape in Ref. 47 is included, the numbers indicated by an asterisk change to 0.166 and 0.566, respectively.

Classical phenomenology	$T=4$ K	$T=6$ K	$T=8$ K
(1) Noninteracting solitons	0.0009	0.036	0.226
(2) Noninteracting solitons including out-of-plane and spin-wave interference correction factors	0.001	0.038	0.197*
(3) Two magnons	0.100	0.225	0.400
(4) Classical analytic results [sum of (2) and (3)]	0.101	0.263	0.597*
CTM results	0.094	0.298	0.504

contributions. Starting from the classical description, the claim is that at sufficiently low temperatures the simple noninteracting soliton result quoted above can be improved to give quantitative results; the improvements consist in correction factors for out-of-plane fluctuations, interference effects with spin waves, and quantum effects. The present numerical results offer an opportunity to check this claim and thus to assess more solidly the validity of the phenomenological soliton description. At the classical level this is possible within an error bound of the order of 10% (data for $B=1$ T are given in Table I); in the quantum case the ambiguity is larger: Whereas the classical correction factors will continue to apply, we have in addition the reduction due to the decrease in effective in-plane spin component, and it is not clear to what degree this quantum correction factor is multiplicative. When we take this quantum correction at $T=0$ as calculated recently,[44] we reproduce the general decrease by a factor of 2 from quantum effects as seen in the numerical results (see Table II). Whereas this is by no means a quantitative confirmation of the phenomenological approach, it should be considered a reasonable guide to an estimate of the soliton-related contribution to the central peak. Since only half of the two-magnon contribution is in the central peak, we conclude that solitons and two-magnon processes contribute equally to the central peak for a field of 1 T and a temperature of 8 K. This should be a lower bound for the soliton part at higher temperatures, since the two-magnon part no longer represents the analytical contributions at higher

TABLE II. Contributions to the quantum structure factor at zero wave number $\mathcal{S}^{xx}(0)$ with a field $B=1$ T applied along the x axis.

	$T=6$ K	$T=8$ K
(1) Solitons	0.02	0.11
(2) Two magnons	0.10	0.18
Sum of (1) and (2)	0.12	0.29
QTM results	0.12	0.256

temperatures, which will decrease stronger than the soliton strength.

For a quantitative comparison to the results of neutron-scattering experiments on $CsNiF_3$, it is most useful to present the results of the numerical calculations in units of the low-temperature spin-wave intensity, since this quantity can be measured without ambiguity.[46] At $q=0$ we can assume that the one-magnon intensity is given directly by $\mathcal{S}^{yy}(0)$. In Ref. 46 the experimental central-peak intensities are given in units of the spin-wave intensity at $T=2$ K, which unfortunately is not within the range of our numerical calculations. Therefore, this intensity was estimated by extrapolating the QTM results presented in Fig. 10(b) down to $T=0$, using as a guide to the low-temperature behavior the results of Ref. 30. This allows us to express the experimentally measured central-peak intensity in the units applied in Fig. 10(a), without any adjustable parameter. The experimental value at $T=12$ K is $\mathcal{S}^{xx}(0)=0.3$, whereas the numerical calculation gives 0.43. The numerical value has to be larger than the experimental one since the latter includes the central-peak contribution only, whereas the QTM calculation also includes the high-frequency two-magnon contribution. Taking this into account and assuming as discussed above that the strengths of the three contributions to $\mathcal{S}^{xx}(0)$ (soliton, low-frequency two-magnon, high-frequency two-magnon) are equal, agreement is again obtained within about 10%. In view of the large uncertainties related to the disentangling of the various contributions to $\mathcal{S}(q)$, this is all that can be expected. Moreover, the temperature variation of the numerical results is in qualitative agreement with the data presented in Ref. 46 and shows a maximum at about the correct temperature.

V. CONCLUSIONS

On basis of the comparison of QTM results with experimental data on $CsNiF_3$, we conclude that the spin Hamiltonian (1) provides an accurate description of the individual chains in this compound for $g=2.1$, $J/k_B=25$ K, and $D/k_B=7.7$ K. Systematic deviations between the numerical and experimental results are found, which extend up to several degrees kelvin above the 3D ordering temperature and are attributed to the coupling between the chains. Attempts to include this coupling within a simple mean-field approximation did not yield satisfactory results, probably because of the presence of competing interchain-interaction mechanisms.

Comparison of results of QTM calculations with those of the classical sine-Gordon model and classical transfer-kernel calculations qualitatively corroborates the physical picture describing the nonlinear excitations in $CsNiF_3$ in terms of solitons. However, it is obvious that the sine-Gordon model has to be extended by including quantum effects and spin components out of the easy plane in order to obtain quantitatively acceptable results. At temperatures below 10 K, satisfactory agreement between such a phenomenological theory and QTM is found, which supports the interpretation of neutron-scattering experiments on $CsNiF_3$ in terms of the extended sine-Gordon model.

Concluding, we note that for both $s=\frac{1}{2}$ and 1 systems the static properties such as heat capacity, magnetization, susceptibility, and spin-spin correlation functions can be accurately calculated by the QTM down to values of the reduced temperature $k_BT/Js(s+1)\approx 0.08$. Nevertheless, a quantitative evaluation of the time-dependent properties, including the specific elementary excitations, still requires an enormous theoretical effort.

ACKNOWLEDGMENTS

We gratefully acknowledge M. Steiner for encouragement and many helpful discussions. Our thanks go also to M. Böhm for helpful remarks and to A. P. Ramirez and W. P. Wolf for sending us their experimental data. This work was supported in part by the Deutsche Forschungsgemeinschaft.

*Present address: Seimens-Nixdorf Informationssysteme AG, Otto-Hahn-Ring 6, W-8000 München 83, Germany.

[1]M. Steiner, Solid State Commun. **11**, 73 (1972).
[2]M. Steiner and H. Dachs, Solid State Commun. **14**, 841 (1974).
[3]J. V. Lebesque, J. Snel, and J. J. Smit, Solid State Commun. **13**, 371 (1973).
[4]M. Steiner and J. K. Kjems, J. Phys. C **10**, 2665 (1977).
[5]C. Dupas and J.-P. Renard, J. Phys. C **10**, 5057 (1977).
[6]R. J. Grill, U. Dürr, and R. Weber, Physica B **86-88**, 673 (1977).
[7]Ch. Rosinski and B. Elschner, J. Magn. Magn. Mater. **4**, 193 (1977).
[8]M. Steiner, J. Appl. Phys. **50**, 7395 (1979).
[9]T. de Neef and W. J. M. de Jonge, Phys. Rev. B **11**, 4402 (1975).
[10]G. Kamieniarz and C. Vanderzande, Phys. Rev. B **35**, 3341 (1987).
[11]G. M. Wysin and A. R. Bishop, Phys. Rev. B **34**, 3377 (1986).
[12]H. J. Mikeska, Phys. Rev. B **26**, 5213 (1982).
[13]T. Tsuzuki, Progr. Theor. Phys. Suppl. **80**, 146 (1984).
[14]H. J. Mikeska and H. Frahm, J. Phys. C **19**, 3203 (1986).
[15]H. J. Mikeska, J. Phys. C **11**, L29 (1978).
[16]J. K. Kjems and M. Steiner, Phys. Rev. Lett. **41**, 1137 (1978).
[17]For a recent review, see H. J. Mikeska and M. Steiner, Adv. Phys. **40**, 191 (1991).
[18]T. Delica and H. Leschke, Physica A **168**, 736 (1990).
[19]K. Kopinga, T. Delica, and H. Leschke, Phys. Rev. B **40**, 7239 (1989); J. Appl. Phys. **67**, 5599 (1990).
[20]H. Betsuyaku and T. Yokota, Prog. Theor. Phys. **75**, 808 (1986).
[21]M. Suzuki, Commun. Math. Phys. **51**, 183 (1976).
[22]T. Delica, K. Kopinga, H. Leschke, and K. K. Mon, Europhys. Lett. **15**, 55 (1991).
[23]T. Delica, Phys. Rev. B **37**, 9879 (1988); T. Delica, R. W. Gerling, and H. Leschke, J. Phys. (Paris) Colloq. **49**, C8-1585 (1988).
[24]It is well known that the susceptibility $\chi^{\alpha\alpha}$ can also be calculated from the canonical spin-spin correlations according to

$$\chi^{\alpha\alpha}=(g^2\mu_B^2/k_BT)\sum_n\int_0^1 d\tau(\langle e^{\tau H/k_BT}S_0^\alpha e^{-\tau H/k_BT}S_n^\alpha\rangle - \langle S_0^\alpha\rangle\langle S_n^\alpha\rangle) .$$

Although the right-hand side is in general different from the expression

$$(g^2\mu_B^2/k_BT)\sum_n(\langle S_0^\alpha S_n^\alpha\rangle-\langle S_0^\alpha\rangle\langle S_n^\alpha\rangle)$$

used in Ref. 19, we have found the difference to be negligible down to all temperatures which are accessible to the QTM; see also T. Sakaguchi, K. Kubo, and S. Takada, J. Phys. Soc. Jpn. **54**, 861 (1985).

[25]J. M. Loveluck, S. W. Lovesey, and S. Aubry, J. Phys. C **8**, 3841 (1975).

[26]M. Blume, P. Heller, and N. A. Lurie, Phys. Rev. B **11**, 4483 (1975).

[27]F. Boersma, W. J. M. de Jonge, and K. Kopinga, Phys. Rev. B **23**, 186 (1981).

[28]M. G. Pini and A. Rettori, Phys. Rev. B **29**, 5246 (1984).

[29]T. Delica and H. Leschke, Physica A **168**, 768 (1990).

[30]E. Allroth and H. J. Mikeska, Z. Phys. B **43**, 209 (1981).

[31]D. J. Scalapino, Y. Imry, and P. Pincus, Phys. Rev. B **11**, 2042 (1975); R. L. Carlin and A. J. van Duyneveldt, *Magnetic Properties of Transition Metal Compounds* (Springer, Berlin, 1977).

[32]A. P. Ramirez and W. P. Wolf, Phys. Rev. Lett. **49**, 227 (1982).

[33]A. P. Ramirez and W. P. Wolf, Phys. Rev. B **32**, 1639 (1985).

[34]M. Steiner, J. Villain, and C. G. Windsor, Adv. Phys. **25**, 87 (1976).

[35]K. Kakurai, Ph.D. thesis, Technische Universität Berlin, 1984.

[36]K. Kakurai and M. Steiner, J. Magn. Magn. Mater. **31-34**, 1215 (1983).

[37]T. Schneider and E. Stoll, Phys. Rev. B **22**, 5317 (1980).

[38]K. Sasaki and T. Tsuzuki, Solid State Commun. **41**, 521 (1982).

[39]J. A. Krumhansl and J. R. Schrieffer, Phys. Rev. B **11**, 3535 (1975).

[40]O. G. Mouritsen, H. J. Jensen, and H. C. Fogedby, Phys. Rev. B **30**, 498 (1984).

[41]A discussion about out-of-plane spin components and quantum effects for a spin-$\frac{1}{2}$ chain can be found in A. M. C. Tinus, K. Kopinga, and W. J. M. de Jonge, Phys. Rev. B **32**, 3154 (1985). From this study, the existence of a competition between these two contributions was concluded.

[42]R. Giachetti and V. Tognetti, Phys. Rev. Lett. **55**, 912 (1985).

[43]M. D. Johnson and N. F. Wright, Phys. Rev. B **32**, 5798 (1985).

[44]H. J. Mikeska, Z. Phys. B **78**, 57 (1990).

[45]G. Reiter, Phys. Rev. Lett. **46**, 202, 518(E) (1981).

[46]M. Steiner, K. Kakurai, and J. K. Kjems, Z. Phys. B **53**, 117 (1983).

[47]C. Etrich and H. J. Mikeska, J. Phys. C **21**, 1583 (1988).